

Innovative Time-Domain Fault Detection Algorithm For Half-Wavelength Transmission Lines: A Contribution To Research And Development Management And Power System Reliability

Marcel Souza Mattos, Ghendy Cardoso, Jr., and Adriano Peres de Morais¹

¹(Graduate Program in Electrical Engineering, Federal University Of Santa Maria – UFSM, Brazil)

Abstract

This paper presents a novel algorithm, monitored by a terminal and based on traveling waves, developed to detect faults in transmission lines slightly longer than half a wavelength. The algorithm demonstrates the ability to identify all fault types while remaining resilient to power oscillations, including the unprecedented capacity to discern faults occurring during such oscillations. The system was modeled in ATP software and the methodology implemented in MATLAB, applying the Karrenbauer transform to decouple current signals and the Teager energy operator to extract incident traveling wave signals. Extensive tests were conducted, covering a wide range of fault types, incidence angles, fault resistances, and power oscillations. The results confirm the method's efficiency, robustness, and ease of implementation. Beyond the technical achievements, this study also highlights its contribution to Research and Development Management and Innovation in Energy Systems, by demonstrating how advanced fault detection can support strategic decision-making, enhance risk management practices, and foster innovation in power system reliability.

Keywords: Research and Development Management, Innovation, Strategic Management, Business Policy, Distance Protection, Fault Detection, Half-Wavelength Lines, Power Swings, Traveling Waves, Teager Energy Operator.

Date of Submission: 17-08-2025

Date of Acceptance: 27-08-2025

I. Introduction

The growing demand for electric energy, particularly in major load centers, combined with the indirect relationship between energy resources and consumption centers, has made it necessary to interconnect transmission lines over long distances to ensure system reliability. Currently, this is achieved using high-voltage direct current (HVDC) lines with converter substations or conventional alternating current (AC) lines with interconnection substations and reactive compensation systems. However, non-conventional solutions are being explored to transmit energy over long distances. Power systems with connections slightly longer than half a wavelength (HWL+) emerge as a viable alternative due to their suitability for long-distance transmission and high capacity, as discussed in (Hubert and Gent, 1965; Prabhakara et al., 1969; Sun et al., 2017; Portela et al., 2007; Jia et al., 2019). Additionally, HWL+ lines present technical and economic advantages, such as the elimination of intermediate substations and reduced need for compensation reactors. From a Strategic Management perspective, the deployment of HWL+ lines represents a business policy decision that balances infrastructure investment, risk management, and innovation opportunities in the power sector (Heij et al., 2020). From a business and strategic management standpoint, HWL+ lines also represent innovation in infrastructure planning, influencing business policies, investment models, and long-term energy strategies.

Studies on HWL+ lines date back to the 1930s and culminated in a field test in the 1960s (Hubert and Gent, 1965; Prabhakara et al., 1969). In Brazil, research began in the 1980s and 1990s to explore the Amazon's potential in collaboration with Eletrobras (Kusel, 2014). More recently, through public calls by ANEEL, universities and power sector companies have been developing studies to improve network geometry and conductor selection, including permanent operation under different load conditions and the development of power electronics devices to connect local systems to HWL lines (Aredes and Dias, 2012; Moreira, 2017; Santos et al., 2011).

In this context, long-distance lines are more susceptible to faults. For safe operation, the protection system must be reliable. Distance protection is widely applied to overhead transmission lines due to its ease of implementation, adjustment, and single-ended operation. This protection operates based on impedance, admittance, or reactance seen by the relay, which are compared to reference values that define protection zones in the RX plane.

Initial studies on HWL+ line protection showed that apparent impedances computed by traditional methods do not exhibit linearity with respect to fault location due to the line's distributed characteristics and capacitive effects (Xiao et al., 2011). Adjustments in apparent impedance calculations have been proposed to address these particularities (Kusel, 2014; Lopes et al., 2014; Fabi'an and Tavares, 2013). Moreover, new detection and phase selection algorithms have been suggested using negative sequence matrices and modal transformations (Jimenez et al., 2022; Bertoletti et al., 2023).

Although distance protection schemes have been studied for long lines, there is still a need to evolve algorithms in terms of speed, reliability, and robustness. Undesired relay operation due to generator faults, sudden load changes, line interruptions, or fault clearing is commonly caused by power swings. Improper protection performance in such high-capacity systems can lead to severe instabilities or blackouts. While most commercial relays include blocking features, an ideal solution would involve fault detection algorithms immune to power swings.

Several techniques for detecting and blocking distance relays under power swings have been proposed for conventional lines. However, few studies address power swings in HWL+ lines (Mattos et al., 2022). This gap directly affects protection and relay operation strategies.

To address this, a high-speed method capable of identifying all fault types in different scenarios, without misoperation and ensuring full coverage, is required. This paper presents a novel ultra-fast fault detection method based on traveling wave (TW) theory using single-ended measurements. The algorithm is immune to power swings. It leverages the Karrenbauer transform to decouple the three-phase current system and the Teager Energy Operator (TEO) to extract the signal's energy, analyzing and comparing fault signatures.

The algorithm detects all fault types, including variations in fault resistance and incidence angle, distinguishing forward and reverse faults. The method is immune to power swings and can detect faults during these oscillations.

This paper is organized as follows: Section 2 presents the fundamentals of traveling wave theory, modal transformation, and TEO. Section 3 describes the proposed model in detail. Section 4 discusses the results, followed by the conclusion in Section 5.

II. General Principles

Traveling Waves

In transmission lines, when fault events occur, transient waves are generated. These waves propagate from the point of the event occurrence to the ends of the line, in both directions. At the ends or at some discontinuity, the transient waves undergo changes, where a portion is reflected and another portion is transmitted.

Equation (1) illustrates the two functions that represent traveling waves. These two components show that the function $f_1(t - \sqrt{LC}x)$ has a displacement in the positive direction of x that displaces in the same direction of $e(x, t)$, called the direct wave component, while the function $f_2(t + \sqrt{LC}x)$ displaces in the negative direction of x , called the reverse wave component.

$$e(x, t) = f_1(t - \sqrt{LC}x) + f_2(t + \sqrt{LC}x) \quad (1)$$

The same relationship applies to the current in (2).

$$i(x, t) = 1/Z_0 f_1(t - \sqrt{LC}x) - \frac{1}{Z_0} f_2(t + \sqrt{LC}x) \quad (2)$$

The components of the direct and reverse waves of the electrical quantities under analysis are related by the natural impedance of the line. However, the reflected voltage wave at the junction with a discontinuity can be determined, from an incident wave by the stress reflection coefficient according in (3).

$$\Gamma_{eR} = \frac{Z_L - Z_0}{Z_L + Z_0} \quad (3)$$

Similarly, we can define the current reflection coefficient in (4).

$$\Gamma_{iR} = \frac{Z_0 - Z_L}{Z_L + Z_0} \quad (4)$$

We can thus conclude that (3) and (4) have opposite signs, which justifies the relationship of reverse waves in the discontinuity with opposite polarities.

Karrenbauer Modal Transformation

The Karrenbauer transform is used to desvinculate phase-dependent signals into independent modal signals, and can be applied to current and voltage signals according to (5) (Dong et al., 2008). In the transformation matrix, the aerial modes described as α , β and γ relate the AB, AC and BC phases respectively (Zin et al., 2015; Bertoletti et al., 2023).

$$\begin{bmatrix} 0 \\ \alpha \\ \beta \\ \gamma \end{bmatrix} = \frac{1}{3} * \begin{bmatrix} 1 & 1 & 1 \\ 1 & -1 & 0 \\ 1 & 0 & -1 \\ 0 & 1 & -1 \end{bmatrix} \cdot \begin{bmatrix} A \\ B \\ C \end{bmatrix} \quad (5)$$

This transformation is a fundamental tool in modal analysis and is particularly effective in high-speed fault detection schemes, as it isolates wave components that can be analyzed individually. Such decoupling enhances the robustness and clarity of the signal processing step, which is essential for systems relying on traveling wave techniques.

Teager Energy Operator (TEO)

The operator calculates the energy required to generate a signal through the relationship between the variation in frequency and amplitude of the signal. When applied to non-stationary signals it is possible to obtain the enhancement of the instants of abrupt variations of the signal (Teager and Teager, 1990; Kaiser, 1990). The operator is defined in (6).

$$\Psi(x(t)) = \dot{x}(t)^2 - x(t)\ddot{x}(t) \quad (6)$$

Equation (6) describes the continuous mode of the TEO, with $\dot{x}(t)$ representing its first-order derivative and $\ddot{x}(t)$ representing the second-order derivative. On the other hand, in discrete mode, this representation is presented in equation (7).

$$\Psi(x(n)) = x[n]^2 - x(n-1)x(n+1) \quad (7)$$

The TEO maintains its independence from the initial phase and, at the same time, is symmetrical and exhibits a quick response to variations in frequency and amplitude. Moreover, its robustness is remarkable even when crossing zero, as it does not require division operations. This operator demonstrates outstanding temporal resolution, as it requires few samples to calculate energy at each instant, highlighting its ability to adapt to abrupt changes (Boudraa and Salzenstein, 2018).

III. Proposed Algorithm

The proposed methodology is based on the analysis of voltage and current magnitudes obtained through Capacitive Voltage Transformers (CVTs) and Current Transformers (CTs), respectively. However, the development of the algorithm discussed in this paper is entirely evaluated based on current magnitudes, whereas voltage magnitudes are only used for signal polarity analysis. Methodologically, this section also illustrates a structured Research Method approach, transforming a technical design into a replicable innovation framework that integrates with Research and Development (R&D) Management practices (Černe et al., 2024).

It is widely recognized that CVTs require careful measurements, especially during transient periods, since overvoltages may compromise the relay's performance and proper operation. Nevertheless, as demonstrated by Guzmán et al. (2017), even when voltage waveforms are attenuated under these conditions, the signal polarity is preserved due to the parasitic capacitances inherent to CVTs.

A Savitzky-Golay smoothing filter is used to eliminate noise and prevent aliasing. The Karrenbauer transform is applied to decouple phase-dependent components, converting them into independent propagation modes. Fault detection is performed using the Teager Energy Operator (TEO).

The output from the aerial mode with the highest magnitude is compared to a defined threshold, which enhances the algorithm's robustness. The fundamental principle behind using the TEO lies in its ability to highlight abrupt signal variations in the time domain, since the method considers instantaneous changes in both amplitude and frequency.

The threshold is defined based on the initial TEO sample values, within approximately 10 ms, where the standard deviation of the TEO samples is compared to the highest TEO value within that window. If the ratio between the highest value and the standard deviation exceeds 20, a fault is characterized. Otherwise, this maximum value is stored for a new test. The next test uses the same ratio but replaces the standard deviation value with the one stored in the previous test. If the condition is met, a fault is confirmed.

This threshold definition was validated through an extensive series of simulations that included noise, power oscillations, sudden load variations, switching operations, and energization events. Thus, the threshold parameter is reliably defined. When energy differentiation is not evident (i.e., the TEO output energy does not exceed the established threshold), the algorithm output characterizes the event as non-fault. Therefore, the algorithm is immune to false fault detections and remains robust against power oscillations.

After the TEO output identifies an event, it is necessary to determine whether the fault is forward or reverse. Faults occurring upstream of the measurement equipment are classified as reverse and should be disregarded. This discrimination is determined by evaluating the first detected point of the traveling wave.

This definition is guided by the connection configuration of the transducers used to acquire the current and voltage signals, from which the signal polarities are extracted at the time of the detected event. According to the traveling wave theory, this classification is given by Equation (8):

$$\text{Forward } \Delta i \times \Delta v < 0, \text{ Backward } \Delta i \times \Delta v > 0 \quad (8)$$

IV. Results And Discussion

Beyond technical robustness, these findings emphasize managerial implications for R&D management, risk control, and business economics in the energy sector. Figure 1 illustrates the test system used to evaluate the proposed algorithm, with detailed network parameters provided in Appendix B. The system was modeled using ATP software, while the algorithm was implemented in MATLAB. The 1000 kV system consists of two sources, and HWL+ line extends for 2592 km, modeled with distributed parameters and line transposition. The signals were sampled at a frequency of 1 MHz.

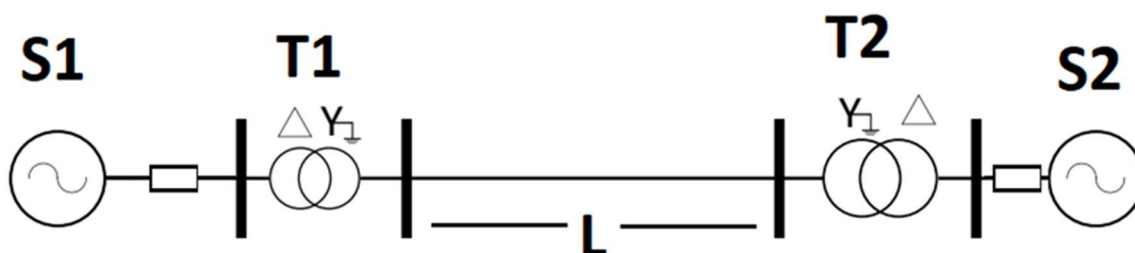


Fig. 1. Test System.

To assess the viability of the fault detection algorithm, a comprehensive set of tests was generated to represent various scenarios commonly found in power systems. Table B.I summarizes the simulated test conditions. From an Operations Management perspective, these results highlight reliability as a strategic element of Risk Management and Business Performance.

Fault locations downstream from the measuring terminal took into account the actual transposition of the transmission line, with four fault sections defined per nine cycles, totaling 36 cases. For upstream faults, events were simulated at 20 km and 200 km from the relay, using a line with identical electrical characteristics to the HWL+.

In all cases, faults were applied across all phases, as well as between phases and ground. For the power oscillation scenarios, the frequency of Source S2 varied relative to Source S1 (60 Hz), as specified in Table A.II. In the fault resistance and incidence angle tests, the values from Table B.I were also applied.

Both forward and reverse fault simulations were executed with a total simulation time of 0.4 s, where the fault was triggered at 0.1 s with a resistance of 0.001 ohm.

Table I. Result for fault detection.

Description of the tests.	Number of tests	Detection	Polarity	Fault	Correct Results
FF	396	396	396	Yes	396
BF	22	22	22	Yes	22
FR	1584	1584	1584	Yes	1584
IA	2376	2376	2376	Yes	2376
PSS	12	No	No	No	12
PSW	12	No	No	No	12
PSS+FF	4752	4752	4752	Yes	4752
PSW+FF	4752	4752	4752	Yes	4752

Table I outlines the variations in tests conducted based on the following case descriptions: FF=Forward Fault, BF=Backward Fault, FR= Fault Resistance, IA= Inception Angle, PSS= Power Swing with S2 (strong), PSW= Power Swing with S2 (weak), PSS+FF= Power Swing Strong + Forward Fault e PSW+FF= Power Swing Weak + Forward Fault.

Forward and Reverse Fault Detection

To examine the impact of fault location along the transmission line, several scenarios were simulated. The variations in distance, as indicated in Table B.I, ensured the occurrence of at least one fault in each transposition cycle, covering all phases. Upstream faults relative to the relay were also considered. In all test cases, the proposed algorithm was able to detect the fault instantaneously and accurately.

Fault Resistance Variation

To evaluate the algorithm under different fault impedance conditions, four additional resistance levels were simulated along the transmission line, as detailed in Table B.I. As the fault resistance increased, the amplitude of the traveling waves (TWs) decreased. Nonetheless, the proposed algorithm maintained its detection performance across all tested resistance values, as shown in Table I.

Fault Incidence Angle Variation

When faults occur with varying incidence angles of voltage, the TW magnitudes experience significant alteration—especially in long transmission lines. In this context, fault scenarios were simulated with different voltage angle incidences to verify the algorithm’s robustness. Results, as presented in Table I, demonstrate that the algorithm consistently detected the fault events. This effectiveness stems from the fact that the Teager Energy Operator is based on analyzing three consecutive samples, thus highlighting energy variations with high temporal resolution.

Power Oscillation

Power oscillations in electrical systems result in noticeable symmetrical changes in the magnitudes of the electrical variables. Unlike fault events that disrupt phase symmetry, power oscillations typically affect all three phases uniformly. However, symmetrical faults may mimic oscillation patterns. To evaluate this behavior, oscillation frequencies for Source S2 were adjusted ± 0.5 Hz from the nominal 60 Hz of Source S1, as shown in Figure 1. Additionally, impedance levels for S2 were varied to simulate both strong (low impedance) and weak (high impedance) sources, based on Appendix A.1 (Santiago and Tavares, 2019).

Table I summarizes the outcomes of the oscillation tests. The algorithm exhibited immunity to power oscillations by not triggering any false fault detections. This result is attributed to the TEO’s frequency- and amplitude-based energy profile, and the detection threshold defined as a function of the initial signal’s standard deviation and maximum TEO energy value. This thresholding approach proved to be a reliable metric for distinguishing between oscillations and true fault events.

Faults Under Power Oscillation Conditions

In this evaluation, the algorithm’s ability to identify the exact onset of a fault during ongoing power oscillation is critical. To test this, faults were simulated under power oscillation conditions. Various scenarios were modeled, combining different oscillation frequencies with fault events, considering two distinct impedance configurations for Source S2. Table I presents the results, which confirm that the algorithm successfully identified the fault onset even in the presence of significant oscillatory behavior.

Faults Near the Measuring Terminal

Some algorithms face challenges in identifying faults located very close to the measuring relay due to the high presence of transients and significant signal energy variations. To assess this limitation, the proposed method was subjected to a set of fault scenarios occurring within 1 km from the measurement terminal. These test cases included all fault types—phase-to-phase and phase-to-ground—as well as variations in fault resistance and the fault inception angle.

Table II. Result for Close-in faults.

Fault Type	Number of tests	Operating results
Forward Fault (l=1km)	11	11 detections
Fault Resistance	44	44 detections
Inception Angle	66	66 detections

The results are presented in Table II and demonstrate the method’s effectiveness in detecting near-terminal faults. The algorithm’s robustness is primarily due to the Teager Energy Operator (TEO), which relies on abrupt energy variations across three consecutive signal samples. Even under adverse conditions, including high-frequency transients, varying resistance levels, and different fault inception angles, the algorithm maintained precise detection performance. These results reinforce the proposed method’s capability to operate effectively even in proximity to the relay, where many conventional techniques may fail.

V. Conclusion

This paper presents a novel time-domain fault detection method for transmission lines based on traveling wave theory and monitored via a single-terminal measurement setup. The algorithm operates in the time domain, enabling ultra-fast performance. Its implementation leverages the Karrenbauer modal transform for decoupling phase-dependent components into independent propagation modes, followed by application of the Teager Energy Operator for event detection. The computational simplicity of the proposed method stems from TEO’s high

sensitivity, requiring only a small number of samples to accurately estimate signal energy variations. Extensive simulation studies validated the algorithm under various fault conditions, including different distances along the half-wavelength line, near-terminal events, fault resistance levels, and inception angles. Additionally, the method was evaluated under power swing scenarios and demonstrated complete immunity to such disturbances. Crucially, it also maintained detection capability during fault events occurring concurrently with power oscillations, evidencing strong selectivity and robustness.

Beyond its technical achievements, this study also provides managerial perspectives on innovation and research and development management in the energy sector. By framing advanced fault detection as a strategic enabler for reliability and risk management, the findings contribute to broader discussions on innovation, infrastructure planning, and decision-making in power systems. Future research may investigate how this framework could be integrated with regulatory policies, long-term investment strategies, and emerging technologies in the electricity sector.

Appendix A. Test system parameters

The characteristics of the line geometry are shown in Fig. A1.

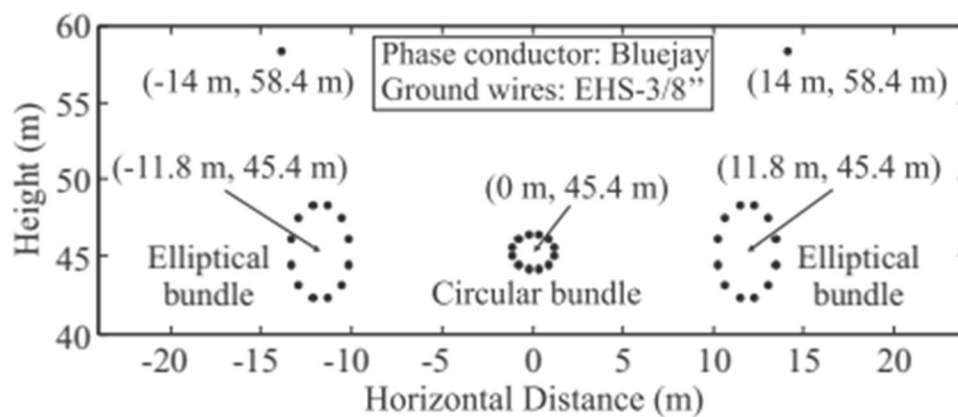


Fig. A1. Cable geometry layout.

In Table A.I, the electrical data of the transmission line are presented, obtained from (Santiago and Tavares, 2019). Table A.II provides the technical data regarding the system sources, adapted from (Lopes et al., 2014). Table A.III illustrates the transformer data, obtained from (Dias et al., 2011).

Table A.I. Transmission Line Parameters.

Line	Resistance		Susceptance		Reactance	
	R0(Ω/km)	R1 (Ω/km)	B0(μS/km)	B1(μS/km)	X0(Ω/km)	X1 (Ω/km)
L	0.0048	0.2856	9.8727	3.4873	0.1689	1.2374

Table A.II. Equivalent Impedances.

Source	Resistance		Reactance	
	R0(Ω)	R1 (Ω)	X0 (Ω)	X1(Ω)
S1	1.6820	0.1635	9.0760	6.7338
S2- Strong	2.9695	1.1864	15	7.1187
S2-Weak	28.868	4.7458	144.34	28.475

Table A.III. Technical data of transformers.

Equipment	Voltage(kV)	Coupling	Power(MVA)	Xt (%)
Transformer1	500/1000	D Yg	5 x 2000	12.0
Transformer2	500/1000	Yg D	5 x 2000	12.0

Appendix B. Tests

Table B.I. Simulation variables used in the tests.

Simulation variables	Defined values
Location Forward Fault (km)	24, 96, 192, 264, 312, 384, 480, 552, 600, 672, 768, 840, 888, 960, 1056, 1128, 1176, 1248,1344, 1416, 1464, 1536, 1632, 17,04, 1752, 1824, 1920, 1992, 2040, 2112, 2208, 2280, 2328, 2400, 2496 e 2568
Location Backward Fault(km)	20 e 200
Fault resistance (Ω)	10, 40, 100 e 200

Fault type	Single-Phase (3) Two-Phase (6) Three-Phase(2)
Variation F2 (Hz)	3.0, 2.5, 2.0, 1.5, 1.0, 0.5, -0.5, -1.0, -1.5, -2.0, -2.5, -3.0
Inception angle (°)	0°, 30°, 60°, 90°, 120° e 150°

Referências

- [1] A. M. Zin, M. Saini, M. W. Mustafa, A. R. Sultan, Et Al. New Algorithm For Detection And Fault Classification On Parallel Transmission Line Using Dwt And Bpnn Based On Clarke's Transformation. *Neurocomputing*, 168:983–993, 2015. Elsevier.
- [2] Guzman, M. V. Mynam, V. Skendzic, J. L. Eternod, And R. M. Morales. Directional Elements—How Fast Can They Be? In *Proceedings Of The 44th Annual Western Protective Relay Conference*, Pages 1–16, 2017.
- [3] O. Boudraa And F. Salzenstein. Teager–Kaiser Energy Methods For Signal And Image Analysis: A Review. *Digital Signal Processing*, 78:338–375, 2018. Elsevier.
- [4] Z. Bertoletti, G. C. Junior, A. P. De Moraes, G. Marchesan, And J. C. Do Prado. Ground And Phase Fault Classification For Half-Wavelength Transmission Lines Relaying Purposes. *International Journal Of Electrical Power & Energy Systems*, 148:108966, 2023. Elsevier.
- [5] F. Kusel. Proteção De Linhas De Transmissão Com Pouco Mais De Meio Comprimento De Onda. *Dissertação De Mestrado, Universidade De Brasília (Unb)*, 2014.
- [6] Portela, J. Silva, And M. Alvim. Non-Conventional Ac Solutions Adequate For Very Long Distance Transmission—Na Alternative For The Amazon Transmission System. In *Proceedings Of The Iec/Cigre UHV Symposium Beijing*, Page 29, 2007.
- [7] C.V. Heij, H.W. Volberda, F.A.J. Van Den Bosch, & Hollen, R.M.A. (2020). How To Leverage The Impact Of R&D On Product Innovation? The Moderating Effect Of Management Innovation. *R&D Management*, V. 50, N. 2, P. 277-294, 2020.
- [8] F. Jimenez, O. Dias, And M. C. Tavares. Fault Classification And Phase Selector Algorithm For Half-Wavelength Transmission Lines. *Electric Power Systems Research*, 203:107637, 2022. Elsevier.
- [9] A. Moreira. Transmissão De Energia A Longas Distâncias Com A Tecnologia Meia Onda: Aspectos Teóricos E Estudos Elétricos. *Transmissão De Energia Elétrica A Longas Distâncias Com A Tecnologia Meia Onda—Aspectos Teóricos & Estudos Elétricos*, 2017. Urutau.
- [10] F.J. Hubert And M.R. Gent. Half-Wavelength Power Transmission Lines. *Ieee Transactions On Power Apparatus And Systems*, 84(10):965–974, 1965.
- [11] V. Lopes, B. F. Kusel, K. M. Silva, D. Fernandes Jr., And W. L. A. Neves. Fault Location On Transmission Lines Little Longer Than Half-Wavelength. *Electric Power Systems Research*, 114:101–109, 2014. Elsevier.
- [12] F.S. Prabhakara, K. Parthasarathy, And H.N. Ramachandra Rao. Analysis Of Natural Half-Wavelength Power Transmission Lines. *Ieee Transactions On Power Apparatus And Systems*, (12):1787–1794, 1969.
- [13] J. F. Kaiser. On A Simple Algorithm To Calculate The 'Energy' Of A Signal. In *Proceedings Of The International Conference On Acoustics, Speech, And Signal Processing*, Pages 381–384, 1990. Ieee.
- [14] J. Jia, J. Yi, A. Wang, W. Lin, W. Zhong, And S. Cheng. Research On The Operation Mode Construction And Stability Control Measures Of Half-Wavelength Transmission Test System. In *Proceedings Of The 2019 Ieee Sustainable Power And Energy Conference (Ispc)*, Pages 252–257, 2019.
- [15] J. Santiago And M. C. Tavares. Analysis Of Half-Wavelength Transmission Line Under Critical Balanced Faults: Voltage Response And Overvoltage Mitigation Procedure. *Electric Power Systems Research*, 166:99–111, 2019. Elsevier.
- [16] J. Sun, M. Li, Z. Zhang, T. Xu, J. He, H. Wang, And G. Li. Renewable Energy Transmission By HvdC Across The Continent: System Challenges And Opportunities. *Csee Journal Of Power And Energy Systems*, 3(4):353–364, 2017.
- [17] M. Teager And S. M. Teager. Evidence For Nonlinear Sound Production Mechanisms In The Vocal Tract. *Speech Production And Speech Modelling*, Pages 241–261, 1990. Springer.
- [18] M. Aredes And R. Dias. Facts For Tapping And Power Flow Control In Half-Wavelength Transmission Lines. *Ieee Transactions On Industrial Electronics*, 59(10):3669–3679, 2012.
- [19] M. Černe, R. Kaše, And M. Škerlavaj. Management Innovations As An Enabler Of Firm Performance, Knowledge Creation, And R&D Initiatives. *Journal Of Management & Organization*.
- [20] M. L. Santos, J. A. Jardini, M. Masuda, And G. L. C. Nicola. A Study And Design Of Half-Wavelength Lines As Na Option For Long Distance Power Transmission. In *Proceedings Of The 2011 Ieee Trondheim Powertech*, Pages 1–6, 2011. Ieee.
- [21] M. S. Mattos, A. P. Moraes, And G. Cardoso Junior. Análise Dos Métodos De Bloqueio Do Relé De Distância Durante Oscilações De Potência Em Linhas De Um Pouco Mais De Meio Comprimento De Onda. *Sepoc 2022*, 2022. Brasil.
- [22] R. Dias, A. Lima, C. Portela, And M. Aredes. Extra Longdistance Bulk Power Transmission. *Ieee Transactions On Power Delivery*, 26(3):1440–1448, 2011. Ieee.
- [23] R. G. Fabi'An And M. C. Tavares. Using Conventional Relays For Protecting Half-Wavelength Transmission Lines From Three-Phase Faults. In *Proceedings Of The International Conference On Power System Transients (Ipst)*, Pages 107–113, 2013.
- [24] S. W. Xiao, Y. J. Cheng, And Ya Wang. A Bergeron Model Based Current Differential Protection Principle For UHV Half-Wavelength Ac Transmission Line. *Power System Technology*, 35(9):46–50, 2011.
- [25] X. Dong, W. Kong, And T. Cui. Fault Classification And Faulted-Phase Selection Based On The Initial Current Traveling Wave. *Ieee Transactions On Power Delivery*, 24(2): 552–559, 2008. Ieee.